Chapter 4

***In Vitro* and *In Silico* Interaction of Porcine α-Amylase with Polyphenols**

from Faba Bean and Evaluation of Antidiabetic activity

4.1. Introduction

Pancreatic α-amylase (E.C. 3.2.1.1) is an enzyme in the digestive system and catalyzes the hydrolysis of starch to a mixture of smaller oligosaccharides consisting of maltose, maltotriose and a number of α (l-6) and α (1-4) oligoglucans (Sudha et al., 2011). The activity of HPA (human pancreatic α-amylase) in the small intestine is related to increase in postprandial glucose levels and the control of which could be a major strategy in the treatment of type-2 diabetes (Eichler et al., 1984).Inhibitors of pancreatic α-amylase delay carbohydrate digestion causing a reduction in the rate of glucose absorption and decrease the postprandial serum glucose levels (Tarling et al., 2008). Some synthetic drugs are available in the market such as acarbose and miglitol which inhibit α-glucosidase and α-amylase. The major side effects of these inhibitors are gastrointestinal problems *viz.* bloating, abdominal problem, diarrhea, and flatulence(Kumar and Sinha, 2012) Previous studies suggest the anti-diabetic and free radical scavenging property of faba beans points out hypoglycemic and antioxidant effect (Tarling et al., 2008). However, the antidiabetic potency of *Vicia faba* seed and their mechanism of inhibition have not yet been extensively studied till now. Therefore, the

objective of the above study is to evaluate the antidiabetic potential of *polyphenols from faba bean* by *in vitro* and *in silico* method.

4.2. Experimental

4.2.1. Seed material

Details about faba and their extraction, purification, characterization were already highlighted in chapter 3.

4.2.2. Chemicals and reagents

Porcine alpha-amylase was purchased from Sigma-Aldrich Co., St Louis, USA, while starch soluble (extra pure) were obtained from Himedia laboratories. Other chemicals and reagents were of analytical grade and water used were distilled.

4.2.3. α -amylase inhibitory assay

The enzyme inhibition studies were performed using a modified procedure of McCue and Shetty, 2004(McCue et al., 2004). The set of tubes containing 500 μl of extract (0.5–5 mg/ml) was kept along with 500 μl of 0.02 M sodium phosphate buffer (pH 6.9) containing α -amylase solution (0.5 mg/ml) in a water bath for 10 min at 25°C. 500 μl of 1% starch solution made in 0.02 M sodium phosphate buffer of pH 6.9 was added at regular interval and further incubated at 25°C for 10 min. The reaction was stopped by adding 500 μl of dinitrosalicylic acid (DNS) reagent. The tubes were kept in boiling water bath for 5 min and cooled to room temperature. 5 ml distilled water was added and the absorbance was measured at 540 nm using a spectrophotometer. Control(acarbose) was made using the same protocol. The α-amylase inhibitory activity was evaluated. Concentrations of extracts resulting in 50% inhibition of enzyme activity (IC_{50}) were determined. The IC_{50} value was defined as the concentration of the extract, containing the

α -amylase inhibitor that inhibited 50% of the PPA activity and calculated by the given formula below:

$$\text{Inhibition}(\%)=[(\text{Abs}_{540\text{control}}-\text{Abs}_{540\text{sample}})/\text{Abs}_{540\text{control}}] \times 100 .$$

4.2.4. Mode of α-amylase inhibition

The inhibitory activity of seed extract on α-amylase by the seed extract was performed according to the modified method described by (McCue and Shetty, 2004). 500 µL of the extract (5 mg/mL) was added with 500 µL of an alpha-amylase solution and preincubated for 10 min at 25°C in one set of tubes. α-amylase was preincubated with 500 µl of phosphate buffer (pH 6.9) in another set of tubes. 500 µL of the soluble starch solution at increasing concentrations (0.30–5.0 mg/mL) was added to both sets of reaction mixtures to start the reaction. The resulting mixture was again incubated for 10 min at 25°C in boiling water bath for 5 min after the addition of 1000 µL of DNS to terminate the reaction. The amount of reducing sugars was determined by spectrophotometrically at 540 nm using a standard maltose curve and converted to reaction rates. A double reciprocal plot (1/(V) versus 1/(S) where is V is reaction speed and (S) is substrate concentration was plotted. The mode of inhibition of the crude seed extract on alpha-amylase activity was determined by analysis of the double reciprocal (Lineweaver-Burk) plot using Michaelis-Menten kinetics (Kazeem et al., 2013b).

4.2.5. Statistical data analysis

All experiments were performed in 3 different sets with each set in triplicates. These data are expressed as mean ± SD. Values of p ≤ 0.05 which are considered as significant.

4.2.6. *In-silico* analysis

4.2.6.1 Preparation of protein and selection of ligands

School of Biochemical Engineering, IIT(BHU) Varanasi

The three-dimensional (3D) structure of (PDB ID: 1PIF) pig alpha-amylase was retrieved from RCSB protein data bank.Energy minimization was done by using Chimera 1.10.2. Based on literature (Kawakami et al., 2010; McCue et al., 2004) and other characterizations such as chemo-profiling (Chapter 3), we selected gallic acid, ellagic acid, catechin, and epicatechin. Acarbose was selected as a standard drug as a reference molecule.

4.2.6.2. Ligand preparation

Three-dimensional structures of different ligands were retrieved from the PubChem Compound database (http://pubchem.ncbi.nlm.nih.gov). The ID of different ligands were as follows: Gallic acid [CID370], Acarbose [CID10256], Catechin [CID73160], Epicatechin [CID3084390], Ellagic acid [5281855].Their energy forms were minimized, by pyRX virtual screening tool (Dallakyan and Olson, 2015) and were converted to PDB format by the Open Babel 2.3.1(O'Boyle et al., 2011).Minimized energy structure of receptor and ligands are shown as (**Figure 4.1.(a),(b),(c),(d),(e),(f)**)
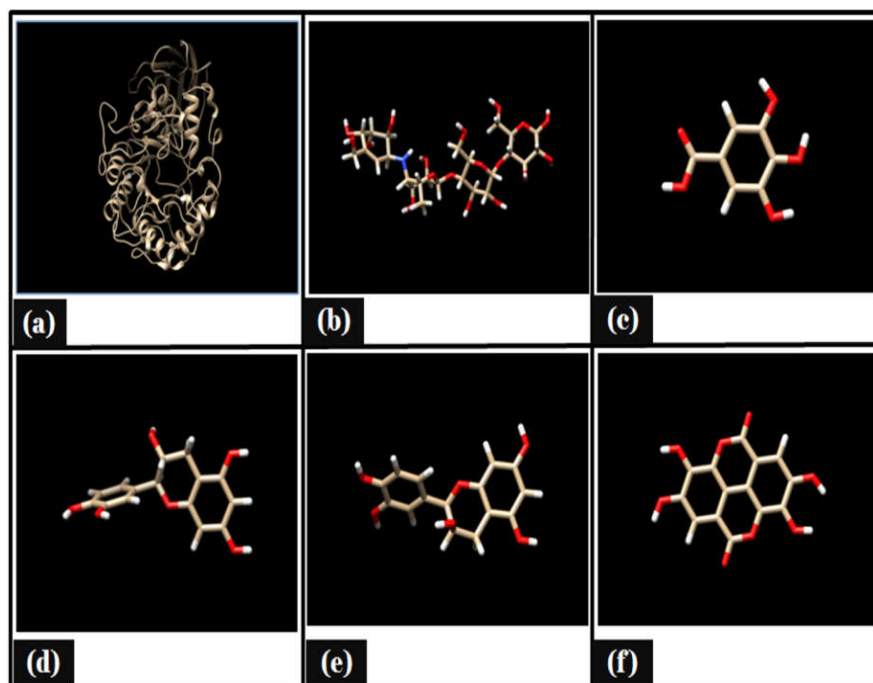
Figure 4.1. Showing minimized energy structure (a) porcine alpha-amylase (b) acarbose (c) gallic acid (d) catechin (e) epicatechin (f) ellagic acid

4.2.6.3. Docking of ligand-receptor procedure

Receptors (alpha amylase (1pif.pdb)) were used for the AudoDock Tools 4.2.0.for docking. Docking was performed by using Autodock 4.2.0 in the interface of MGLTool 1.5.4 (Morris et al., 2009). AutoDock is a fast automatic docking tool and considered as the best docking method to predict the free energy of binding.The grid maps represents the ligand in real docking target site were calculated with gid box dimension of $60 \times 60 \times 60$ Å and spacing of 0.375 Å by taking the centre of the ligand as the centre of the grid. Algorithm parameter for docking constitutes the population in the genetic algorithm was 50, the number of energy evaluations was 250,000, and the maximum number of iterations was 27,000. AutoDock is based on semiempirical free energy force field to confirm or evaluates actual conformations during docking simulations. Further interaction analysis was done using the autodock tools and visualized by the Chimera1.10.2. To study the intermolecular interactions between the targets and the compounds LigPlot12 were used to plot their interactions from 3D to 2D.

### 4.2.6.4. Molecular dynamic simulation analysis

Molecular dynamics (MD) simulation of 50 ns was carried out by using GROMACS version 4.6.7 under gromos 53a6 force field (Oostenbrink et al., 2004; Van Der Spoel et al., 2005). Each complex was simulated compared against the apo form of the enzyme. Moreover, the simulation was repeated one more time for each system. Based on binding energy and their binding energy catechin was selected for molecular dynamic and simulation studies with alpha-amylase. Moreover, the simulation was

repeated one more time for each system. The spc216 water model was recruited for providing the system an appropriate medium (Dyer et al., 2009)**.**

4.3. Results and discussion

### 4.3.1. The inhibitory potency of *Vicia faba* seed extracts against α-amylase activity

(**Figure 4.2**) showed the **α**-amylase inhibition potential of the *Vicia faba* seed extracts (0 to 5 mg/ml). Maximum inhibition percentage was found in acetone extract (88.3%) with respect to control (93.5 %). Extrapolation of α-amylase effectiveness from the dose-response curve showed that acetone extract contained the most efficient α-amylase inhibitor with an IC_{50} value of 2.94 mg/ml. This could be one of the several strategies adopted in Diabetes mellitus treatment. The inhibition of digesting enzymes α-amylase may lead to lower down postprandial glucose level and this is an effort to search for alternative drugs from medicinal plants with efficient potential and lesser side effects than synthetic drugs(Kazeem et al., 2013a).

9
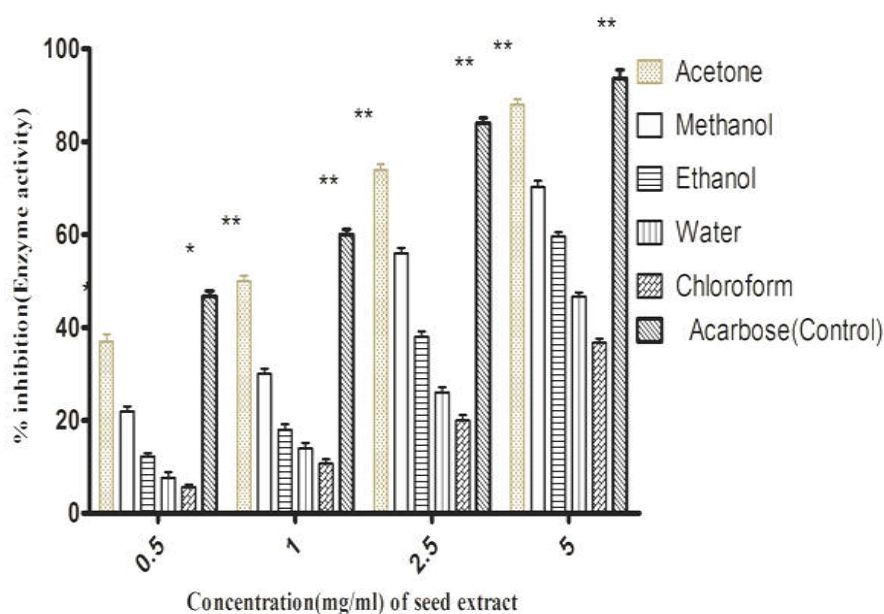
Figure 4.2. The inhibitory potency of alpha-amylase against different seed extracts at various concentrations.

4.3.2. Mode of enzyme inhibition and their kinetic analysis

(**Figure 4.3**) showed that the enzyme follows Michaelis-Menten kinetics. To find out the type of inhibition Lineweaver-Burk plot was made for α -amylase activity. It was estimated using starch as substrate and mixed type of the enzyme inhibition was observed (Figure 3.2). It was evident from **Figure 4.3** that Km and Vmax value of acetone extract was found to be 0.56 mM, 0.14 mM/min (Km, Vmax) respectively, Whereas Km and Vmax of standard or reference molecule (acarbose) were found to be 0.40 mM, 0.20 mM/min respectively.
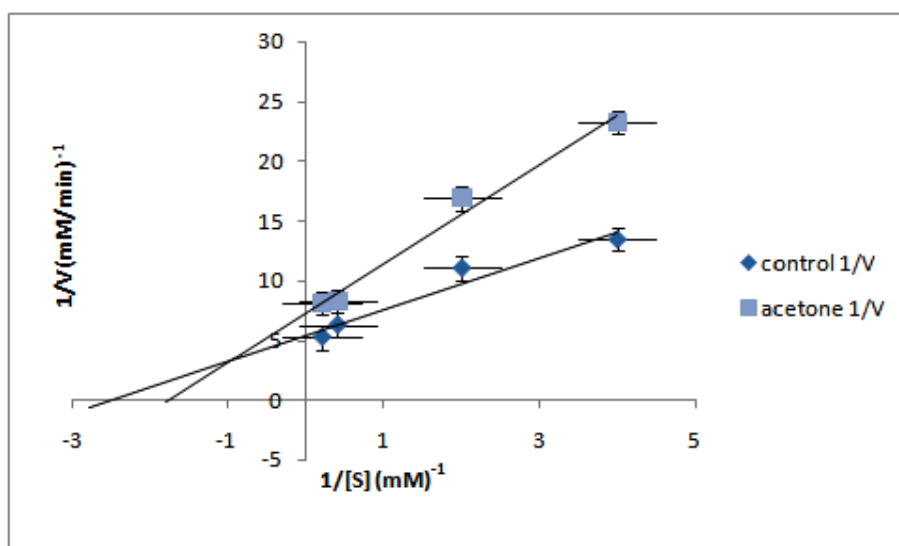
 Figure 4.3. Mode of inhibition of alpha-amylase by acetone seed extract (Lineweaver-Burk plot).

Kinetic analysis showed that inhibition is a combination of competitive and non-competitive enzyme inhibition. These findings supported the reports indicating that

excessive inhibition of pancreatic alpha-amylase could result in the bacterial fermentation of undigested carbohydrates and therefore mild alpha-amylase inhibitory activity is desirable (Apostolidis et al., 2007). Mixed type of inhibition in LB plot confirmed that the active components in the extract might not compete with the substrate for binding to the active site rather the inhibitors may bind to a separate site on the enzyme to delay the conversion of disaccharides to monosaccharide(Mogale et al., 2011; Ogunwande et al., 2007). This mixed type inhibition kinetics is specific of some medicinal plants, due to the variety of phytochemicals present in the extract and may be acting in different ways (Mills and Bone, 2000). The findings made are in confirmatory of other studies on alpha-amylase and alpha-glucosidase inhibitors of different medicinal plants. The potential inhibitors from plants mainly belong to flavonoids class which has features of inhibiting α-amylase and α -glucosidase activities (KWON et al., 2007).

4.3.3. Molecular docking studies

The molecular docking tool can be exploited to study the interaction between a small molecule and a receptor at the atomic level, which may give the insight to characterize the behavior of small molecules in the binding site of target proteins as well as to elucidate fundamental biochemical processes (McConkey et al., 2002).

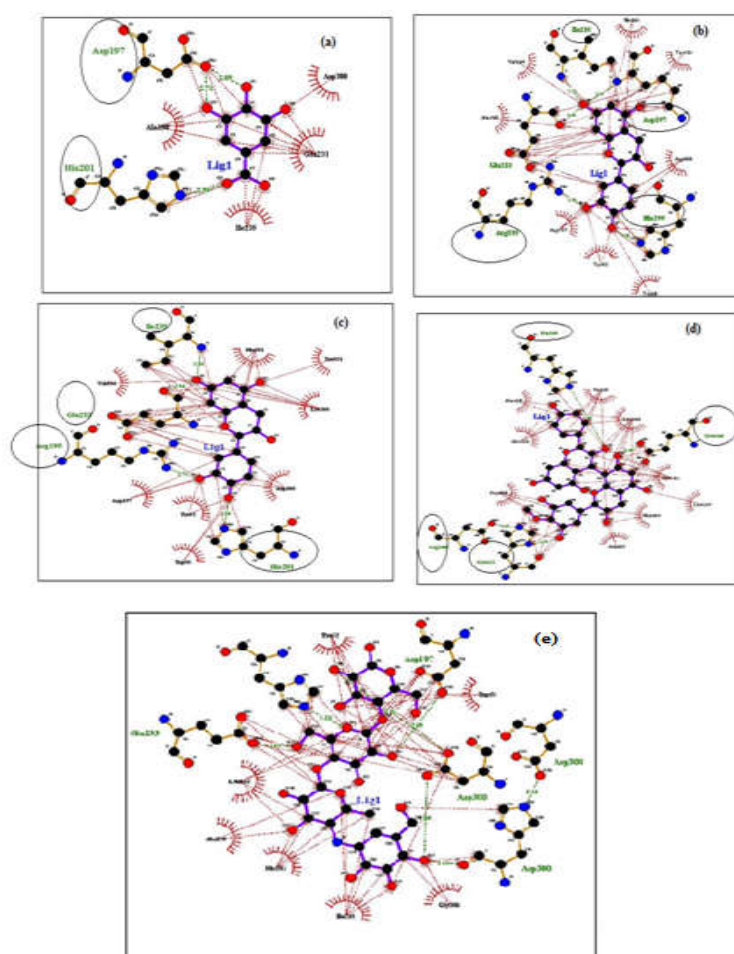**Table 4.1:** Docking analysis of different ligands with porcine alpha-amylase

| Compound	Binding energy	Number of hydrogen	Amino acid participated in hydrogen bonding
Acarbose	-5.29	4	Asp197,Asp300,Glu233,Asp300
Gallic acid	-5.43	3	His201,Asp197,Asp300
Ellagic acid	-6.39	5	Asp300,Glu233,His201,Glu240,Tyr195

School of Biochemical Engineering, IIT(BHU) Varanasi

Catechin	-6.76	5	Glu233,Arg195,His201,Ile235,Asp197
Epicatechin	-6.45	5	Glu233,Arg195,His299,Ile235,Asp197

Three interacting catalytic binding sites of porcine α-amylase (catalytic triads of Asp197, Glu233, Asp300) were identified (Uitdehaag et al., 1999). The docked stable confirmation showed binding energy in the range of −5.29 to −6.56 Kcal/mol (**Table 4.1**). The 2D view of protein-ligand interactions was generated by lig plot(Wallace et al., 1995). Lig plot (**Figure 4.4**) and autodock tool interaction analysis(Sanner, 1999)

Figure 4.4. Lig plot showing hydrogen bonding and hydrophobic interaction in different ligands (a) acarbose (b) epicatechin (c) gallic acid (d) ellagic acid (e) catechin with porcine alpha-amylase.
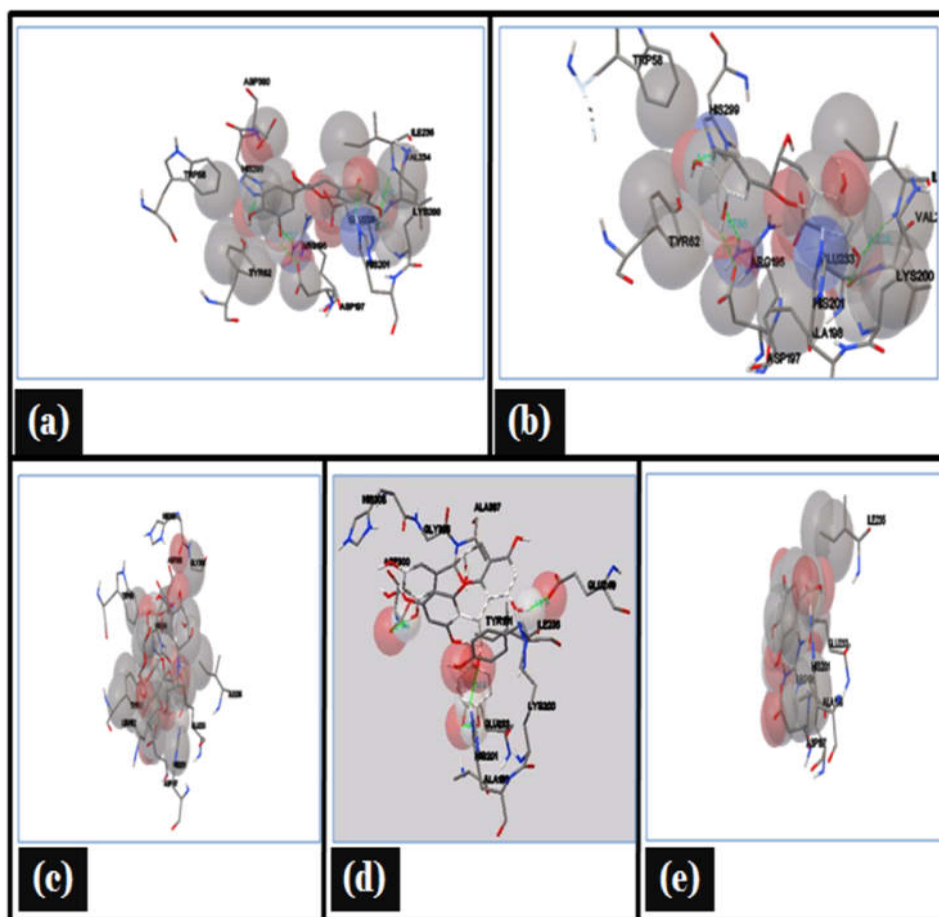
Figure 4.5. Showing autodock tool analysis of different types of interaction in different ligands (a) catechin (b) epicatechin (c) acarbose (d) ellagic acid (e) gallic acid with porcine alpha-amylase.

(**Figure 4.5**) showed different residues such as Glu233, Arg195, His201, Ile235, ASP197 present on the catalytic site of α-amylase interacted with ligands. A standard drug acarbose exhibit hydrogen binding with amino acid residues Asp197, Asp300,

Glu233 which directly participate in the catalytic activity of this enzyme. The docking studies showed that the van der Waals, electrostatic and desolvation energies play an important role in binding. The hydrophobic interactions were formed by Val234, lys200, Val163, leu165, Ser191, Asp197 in acarbose with porcine alpha- amylase molecule. Faba bean polyphenolic compound showed more negative binding energy in comparison to a standard drug as acarbose. Above results were in agreement with the literature, it showed that non-covalent interactions occur between polyphenols and enzymes (Siebert et al., 1996). Hydroxyl groups and galloyl groups are present in the molecular structure of polyphenols (He et al., 2007) and that is responsible for hydrogen bonding with the polar amino acid of an enzyme. Galloyl groups in polyphenols are responsible for hydrophobicity (He et al., 2006) and therefore, polyphenols can interact with enzymes through hydrophobic association. The galloyl moiety may play a crucial role in interaction with mammalian α-amylase its positions in aromatic ring mostly affect the effectiveness (Koh et al., 2009). The combined effects of hydrophobic interaction and hydrogen bond formation between polyphenols and the porcine-alpha amylase could contribute to control postprandial hyperglycemia in type 2 diabetic patients. It was observed that the structure catechin exhibits binding energy of -6.56 Kcal/mol and the acarbose as a standard drug exhibits binding energy of -5.29 Kcal/mol. The binding energies (ΔG_{BE}) of the all best- docked molecule were given in (**Table 3.1**).

4.3.4. Root mean square deviation

Stability of the trajectory of Cat:α- amylase was evaluated on the basis of root mean square deviation (RMSD) and **Figure 4.6** reports the RMSD of the backbone atoms for Cat:α- amylase where values seem deviated from native structure throughout simulation and values lay between ~0.175 nm and 0.275 nm. Consequently, the RMSDs

School of Biochemical Engineering, IIT(BHU) Varanasi

fluctuation difference was found about ~0.1 nm from the starting structure. Furthermore, the approximations of RMSD for backbone atoms represents significantly stable.
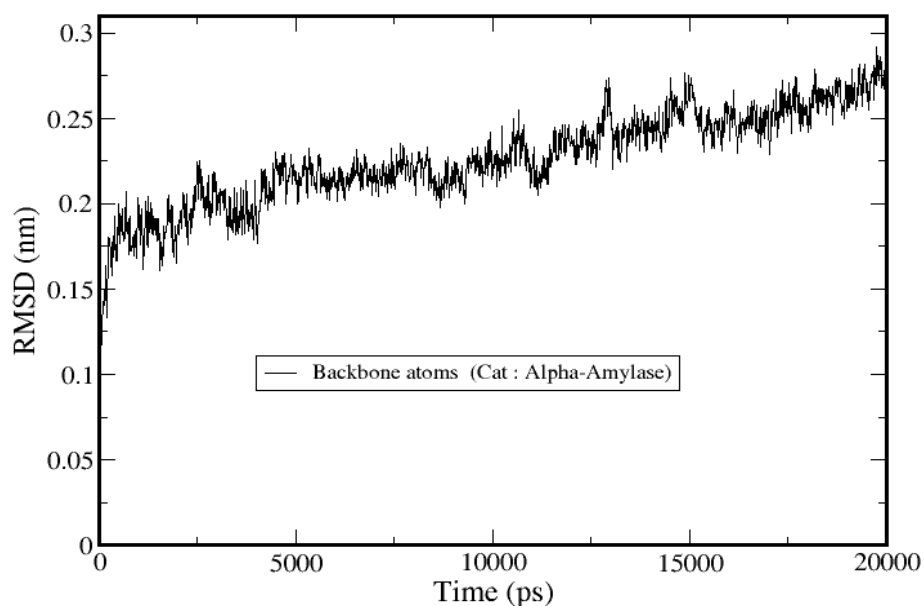

Figure 4.6. Demonstration of Root mean square deviation (RMSD) of protein backbone atoms for Cat:α-amylase complex with respect to the initial structure. Value changes are initiated at the same time pattern, however, both complexes show different fluctuation pattern during simulation. Interestingly, RMSD values of complexes occur in between 0.15 nm to 0.35 nm throughout the simulation and reach a plateau at the end.

4.3.5. Cluster analysis

Cluster analysis was performed for the backbone atom to know the behavior of catechin on α-amylase. Figure **4.7** details the analysis which shows the distributions of clusters by means of representative structures of Cat:α-amylase, possessing significant lifetime duration. Total 12 clusters were found during simulation and the trajectory was subjected to cluster analysis (cut-off value 0.15 nm) to secure convergence and observe

the effect of catechin on α-amylase during simulation. Distributions were provided a larger dominating representative structure **(Figure 4.6)** stayed longer survival time of ~12 ns. This representative cluster was further offered, a rapid equilibrium, sampling a single and robust conformation that does not differ in their stability. However, complex Cat:α-amylase was initially found two more larger clusters, whose life spans were noted from 0 to 4 ns and ~13 to end of simulation time. Although, it resists up to ~3 to 2 clusters respectively (**Figure 4.6**). Cluster distribution was executed less noisy and trajectory exhibits a smooth continuous transition to a new conformational, represented by a series of clusters.
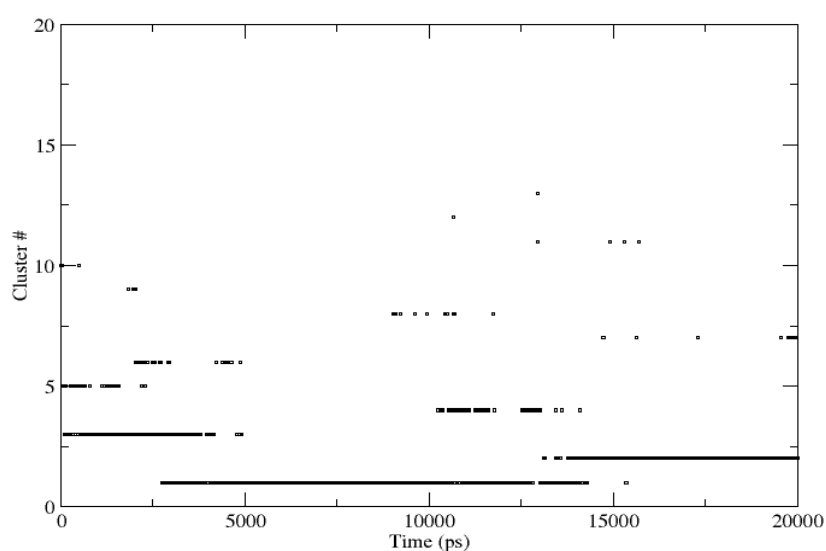

Figure 4.7. Cluster distribution of complex Cat:α-amylase at cut-off 0.15 nm. The life span of the largest cluster was noted from ~2 ns to ~14 ns.

4.3.6. Effect of catechin on α-amylase

The conformational changes were taken place during the stabilization of Cat:α-glucosidase complex. It was observed that the catechin was triggered interactions boost during simulation and activation process involves relative motion of the enzyme; a

*School of Biochemical Engineering, IIT(BHU) Varanasi*

process where the pattern of contact between the catalytic residues and catechin are varying.
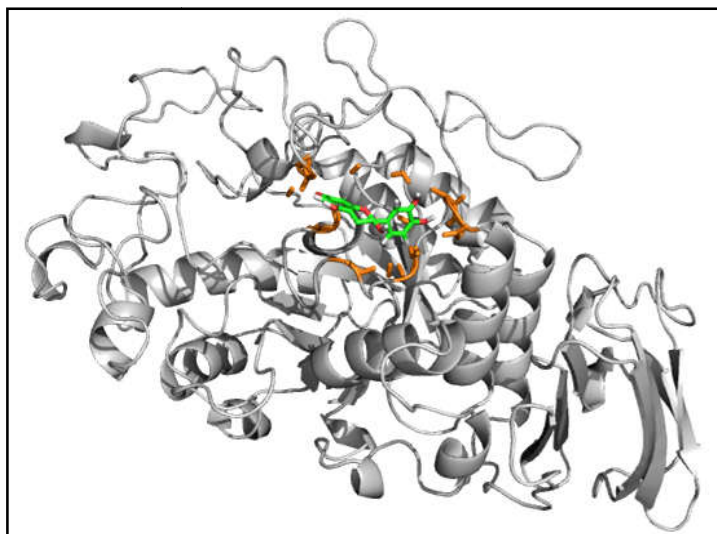
Figure 4.8. Initial (T = 0 ns) of Cat:alpha-amylase complex. The magnifying views of confirmations are provided to highlight the binding residues and position of Catechin during simulation.
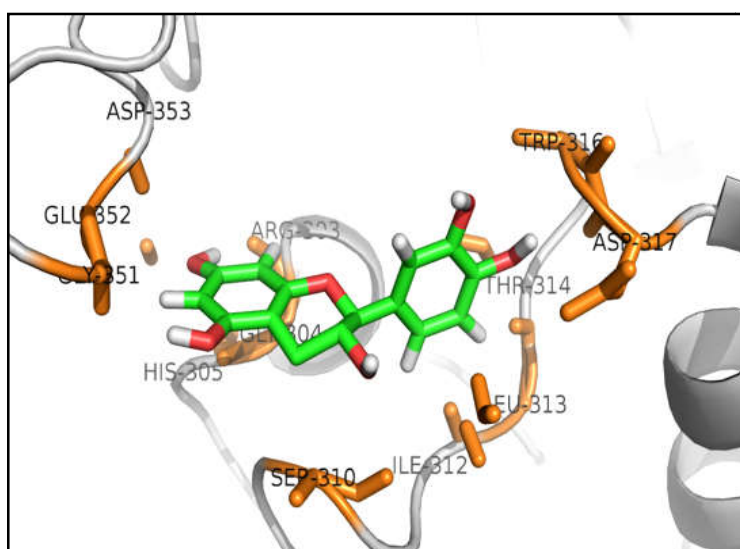
Figure 4.9. Initial (T =20 ns) structure of Cat:alpha-amylase complex represents the catalytic and another crucial residue
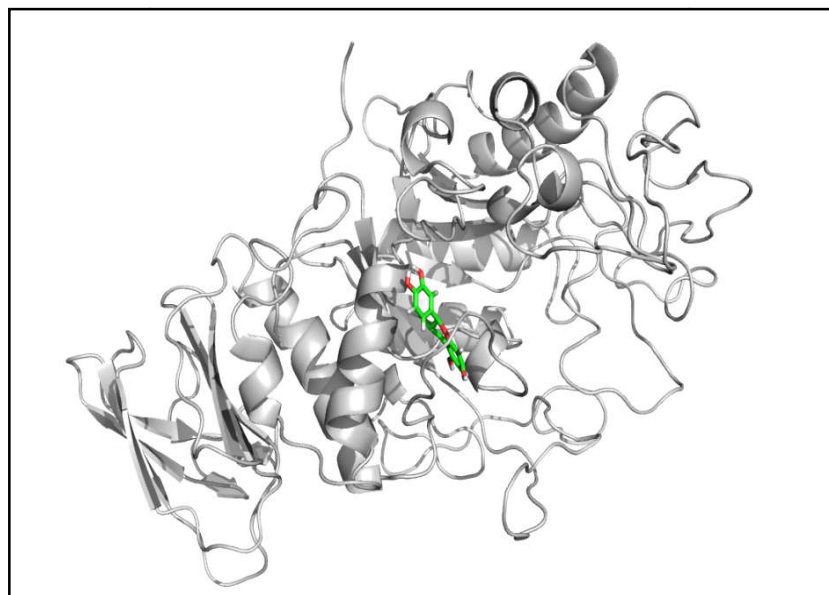
Figure 4.10. Final structure (T = 20 ns) of Cat:alpha-amylase complex. The magnifying views of confirmations are provided to highlight the binding residues and position of catechin during simulation

Figure **4.8,4.9.4.10,4.11** assists the visualization of contacts between catechin and catalytic site residues. Furthermore, magnifying views contribute to review the changes in the binding event during simulation for initial (blue) and final (orange) structure of the complex. In the first observation, the catechin was shifted to gain additional residues during simulation. Moreover, magnifying views clearly represented the α-amylase binding pocket to evaluate the ability of the catechin to interact with the catalytic residues. The residues in noncatalytic regions of the α-amylase enzyme are avoided, however, we have presented the superimposition between the initial and final structure to visualize the catalytic domain conformational changes occurred in α-amylase enzyme during simulation. The interacting residues involved in interaction with catechin

displayed (**Figure 4.8, Figure 4.11**) such as Glu233, Arg195, His201, His305, Ile235, Asp197 Tyr63, Asp326, Phe321, Gln13, Arg197, Trp49, Tyr352 and Ala347.
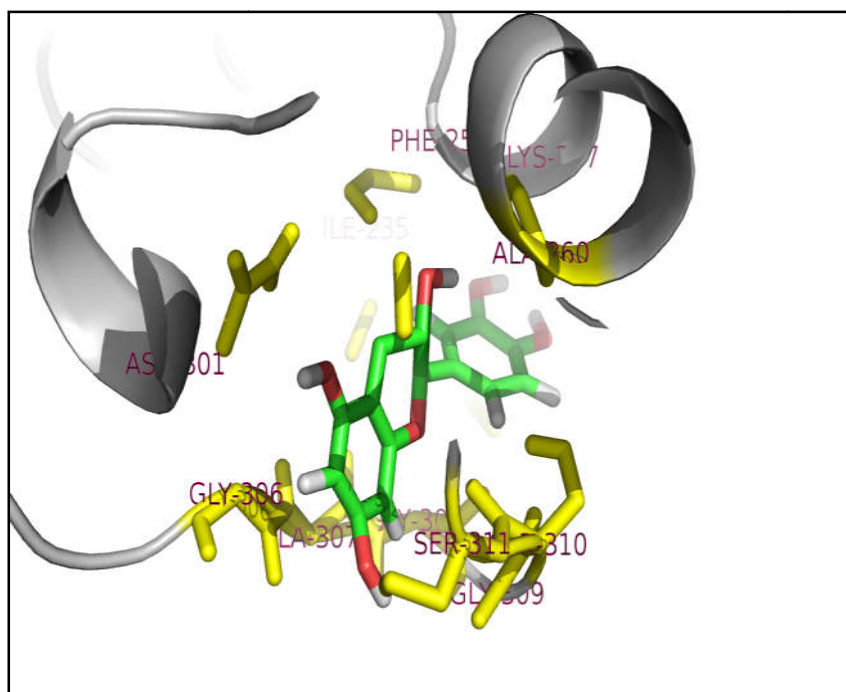
Figure 4.11. last structure (T = 20 ns) of Cat:alpha-amylase complex represents catalytic and other crucial amino acid residue

4.4. Conclusion

Acetone and methanol extract of *Vicia faba* seed displayed most effective inhibition against the α-amylase enzyme. This enzyme activity showed that seed extract suggested the mixed type of inhibition with α-amylase. However, the further *in-silico* study confirmed that polyphenolic compound binds with the catalytic and other residues of α-amylase by hydrogen bonding and hydrophobic interaction. This inhibition of enzyme might be either due to the synergistic effect of the phytochemical constituents of polyphenols present in it or acting separately. Molecular dynamic simulation predicts the

School of Biochemical Engineering, IIT(BHU) Varanasi

interaction between phenolic compounds and digestive enzymes that may be an initial step towards the development of drug, nutraceuticals or functional foods.